Chemistry & Biology
Article

Biosynthesis of the Putative Siderophore Erythrochelin Requires Unprecedented Crosstalk between Separate Nonribosomal Peptide Gene Clusters

Orestis Lazos,[1] Manuela Tosin,[1] Adrian L. Slusarczyk,[1] Steven Boakes,[1,3] Jesus Cortés,[1,3] Philip J. Sidebottom,[2] and Peter F. Leadlay[1,*]
[1]Department of Biochemistry, University of Cambridge, 80 Tennis Court Road, Cambridge CB2 1GA, UK
[2]GlaxoSmithKline Medicines Research Centre, Gunnels Wood Road, Stevenage, Hertfordshire SG1 2NY, UK
[3]Present address: Novacta Biosystems, BioPark Hertfordshire, Broadwater Road, Welwyn Garden City, Hertfordshire AL7 3AX, UK
*Correspondence: pfl10@mole.bio.cam-ac.uk
DOI 10.1016/j.chembiol.2010.01.011

SUMMARY

The genome of the erythromycin-producing bacterium *Saccharopolyspora erythraea* contains many orphan secondary metabolite gene clusters including two (*nrps3* and *nrps5*) predicted to govern biosynthesis of nonribosomal peptide-based siderophores. We report here the production by *S. erythraea*, even under iron-sufficient conditions, of a 2,5-diketopiperazine siderophore candidate we have named erythrochelin. Deletion of the nonribosomal peptide synthetase (NRPS) gene *ercD* within the *nrps5* cluster abolished erythrochelin production. The tetrapeptide backbone of erythrochelin (α-*N*-acetyl-δ-*N*-acetyl-δ-*N*-hydroxyornithine-serine-δ-*N*-hydroxyornithine-δ-*N*-acetyl-δ-*N*-hydroxyornithine) suggests an orthodox colinear model for erythrochelin assembly. Curiously, the δ-*N*-acetyltransferase required for erythrochelin biosynthesis is encoded within a remote NRPS-cluster (*nrps1*) whose own NRPS contains an inactivating mutation. Disruption of the *nrps1* gene *mcd* abolished erythrochelin biosynthesis, which could then be restored by addition of synthetic L-δ-*N*-acetyl-δ-*N*-hydroxyornithine, confirming an unprecedented example of functional crosstalk between *nrps* clusters.

INTRODUCTION

Actinomycete bacteria have been recognized for more than 60 years as highly significant producers of diverse and bioactive secondary metabolites, many of which have entered the clinic as antibiotics, immunosuppressants, anticancer, or antiparasitic compounds. Depending upon the conditions used for growth, many strains are known to be capable of producing more than one metabolite (Bode et al., 2002), often with overlapping or complementary bioactivities (Challis and Hopwood, 2003). However, the full biosynthetic potential of these organisms has remained unknown. Recent genome-scale sequencing of representative filamentous actinomycetes has now revealed that in general each strain houses multiple biosynthetic gene clusters, many of them predicted to encode the assembly-line biosynthesis of complex polyketides or nonribosomal peptides, where the link between the gene sequence and the structure of the inferred chemical product is particularly direct (Clardy et al., 2006; Zerikly and Challis, 2009). Under commonly used laboratory conditions, many of these clusters are apparently silent or, at least, have not been linked to the production of a known compound, and therefore represent an unexploited pool of natural structural diversity. There is great interest in uncovering the products of such orphan clusters, and in learning how they are controlled. Where strains produce multiple natural products, very little is yet understood of how this is orchestrated, either at the transcriptional or the enzymatic level.

A universal feature of actinomycete genomes is the presence of genes for the biosynthesis of iron-scavenging small molecules (siderophores), which commonly are strongly induced under conditions of iron depletion. Iron is an essential element for almost all known micro-organisms, but is mainly present in the environment in an insoluble and unavailable form (Chipperfield and Ratledge, 2000). Therefore, the ability to deploy small molecules to capture and sequester iron from the environment is likely to confer an evolutionary advantage (Wandersman and Delepelaire, 2004). Siderophores have been classified into two groups according to their biosynthetic origin, one NRPS dependent (Crosa and Walsh, 2002) and the other NRPS independent (Challis, 2005). Figure 1 shows the structures of representative hydroxamate siderophores from actinomyces, including the NRPS-dependent fuscachelin A **1** (from *Thermobifida fusca*) (Dimise et al., 2008), and coelichelin **2** (from *Streptomyces coelicolor*) (Lautru et al., 2005) which were both discovered by genome mining. The putative siderophore 2,5-diketopiperazine foroxymithine **3** was first isolated from *Streptomyces nitrosporeus* (Umezawa et al., 1985) and is of unknown biosynthetic origin. NRPS systems catalyze the assembly-line formation of peptides from amino acid building blocks (Sieber and Marahiel, 2005). Each module in an NRPS multienzyme is successively used to elongate the peptide by one amino acid, a feature referred to as colinearity. Each module contains an adenylation (A) domain for the selection and activation of the correct amino acid, a peptidyl carrier protein (PCP) that tethers the growing peptide chain and the incoming aminoacyl unit, and a condensation (C) domain to catalyze peptide bond formation between the PCP-bound species. Optional domains include epimerization (E),

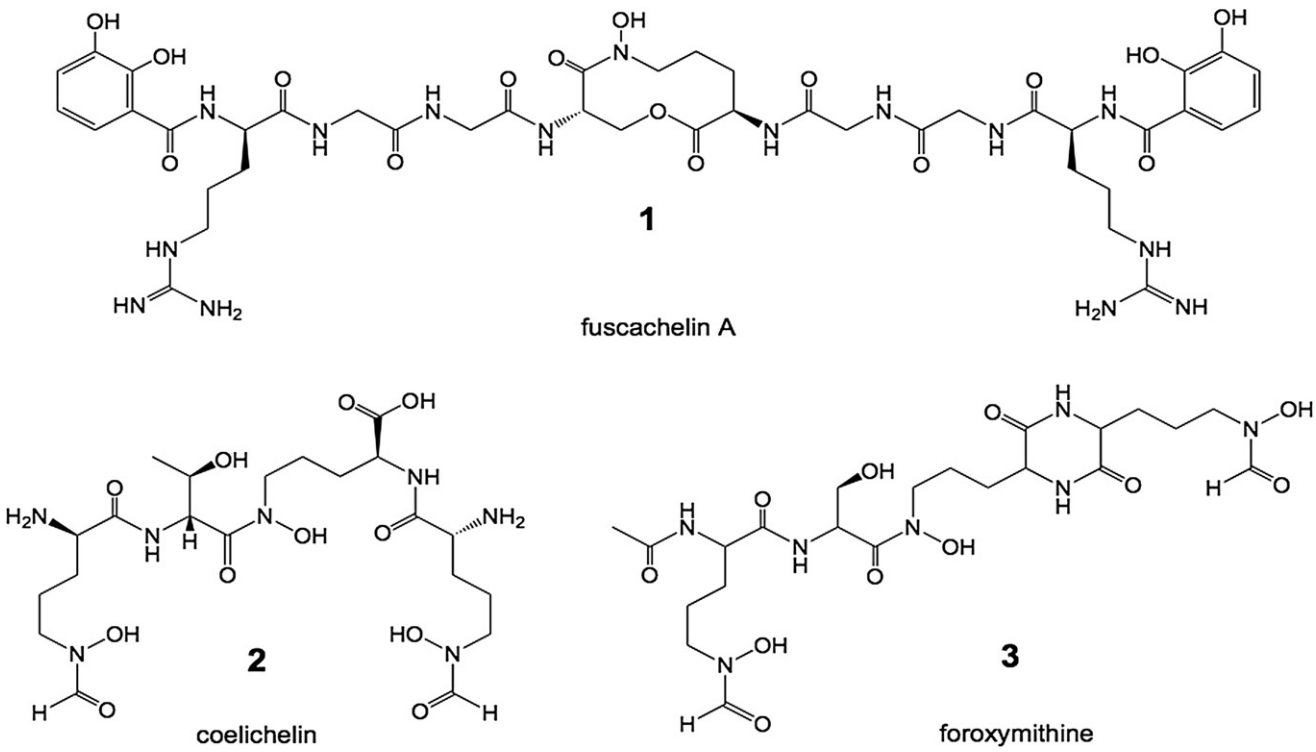

Figure 1. Typical Peptide Siderophores from Actinomycetes

The catechol-containing fuscachelin A **1** and the hydroxamate coelichelin **2** were both discovered by genome mining of NRPS gene clusters. The 2,5-diketopiperazine foroxymithine **3** is of unknown biosynthetic origin.

heterocyclization (Cy), and oxidation (Ox) domains. The full-length NRPS product is normally released by a thioesterase (TE) domain giving rise to free acids, lactones, or lactams. Strikingly, the biosynthesis of both **1** and **2** involves unexpected NRPS enzymology, in which some enzymes are reused and others are skipped (Barry and Challis, 2009).

The Gram-positive filamentous actinomycete *Saccharopolyspora erythraea* NRRL 23338, the producer strain of the macrolide polyketide erythromycin, is also known to produce two other secondary metabolites, rhamnosylflaviolin (which imparts the red color to this organism) (Cortés et al., 2002) and a hydroxamate siderophore of unknown structure tentatively named erythrobactin (Oliveira et al., 2006). However, the recently sequenced and annotated genome (8.2 Mbp) contains as many as 23 orphan biosynthetic operons for the production of secondary metabolites, including one (*pke*) for a very large complex polyketide (Boakes et al., 2004) predicted (Frank et al., 2007) to resemble known aurafuranones (Banskota et al., 2006), and at least seven nonribosomal peptide synthetase (NRPS)–containing gene clusters for the biosynthesis of nonribosomal peptides (Oliynyk et al., 2007). *S. erythraea* appears to rely exclusively on the NRPS pathway for the acquisition of iron, because (unlike sequenced *Streptomyces* strains) its genome contains no genes for the NRPS-independent pathway (Oliynyk et al., 2007) that was first identified for aerobactin biosynthesis (De Lorenzo and Neilands, 1986).

We report here the isolation and structural characterization of erythrochelin, a putative hydroxamate-type siderophore produced by *S. erythraea* that closely resembles foroxymithine **3** and we show that (in contrast to **1** and **2**) its biosynthesis involves an orthodox colinear use of each of the extension modules of the NRPS in the orphan gene cluster *nrps5*. Unexpectedly, however, the gene for an *N*-acetyltransferase required for the production of L-δ-*N*-acetyl-δ-*N*-hydroxyornithine, one of the amino acid building blocks of erythrochelin, was missing from the *nrps5* gene cluster; and was finally located in an entirely separate and apparently defunct NRPS cluster *nrps1*, an unusual example of required functional crosstalk between separate biosynthetic gene clusters.

RESULTS

Isolation and Structural Characterization of Erythrochelin from *S. erythraea*

We first noted the production of a distinct iron-chelating compound by *S. erythraea* when using a mutant strain JC2 (Rowe et al., 1998) from which the genes for erythromycin biosynthesis had been specifically deleted, and which nevertheless showed antibiotic activity against the erythromycin-sensitive Gram-positive organisms *Micrococcus luteus* and *Bacillus subtilis*. (We refer to this compound as a siderophore for convenience but strictly speaking positive identification as a siderophore requires evidence that the iron-chelator complex is taken up by the producing strain). Fractionation of the water-soluble portion of fermentation extracts (Experimental Procedures) was monitored using this bioassay, and led to the isolation of

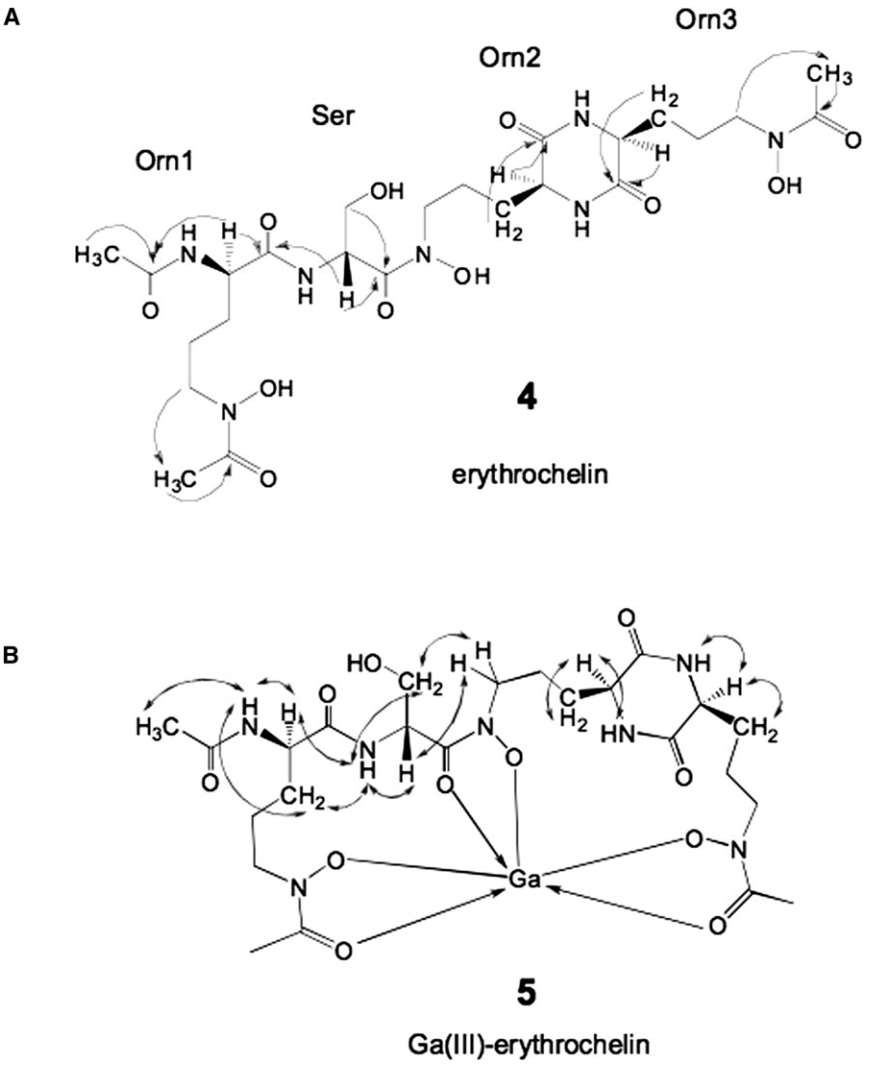

Figure 2. The Structure of Erythrochelin

(A) The structure of *apo*-(iron-free)-erythrochelin as deduced from 1D and 2D NMR analysis (showing the most significant HMBC correlations in CD_3OD). The configuration is deduced from biosynthetic considerations.

(B) Key NOESY/ROESY correlations observed for the Gallium(III) erythochelin complex in DMSO. For further details see Experimental Procedures and Figure S1 in the Supplemental Information.

an apparently new natural product, which retained the antibiotic activity. Preliminary mass spectrometry (MS) and nuclear magnetic resonance (NMR) analysis suggested this was a tetrapeptide potential siderophore of molecular ion *m/z* 604.3 containing one serine and three modified ornithine residues (Boakes, 2002) (specifically, two δ-*N*-acetyl-δ-*N*-hydroxyornithine residues and one α-*N*-acetyl-δ-*N*-hydroxyornithine residue) and we accordingly named this compound erythrochelin.

Subsequently, purification of erythrochelin was carried out more conveniently by monitoring fractionated extracts for the presence of the characteristic $(M + H)^+$ molecular ion at *m/z* 604.3, and of its MS-MS fragmentation pattern (Boakes, 2002) The compound was isolated by passing it successively through a polystyrene divinylbenzene column and a weak anion-exchange column to remove impurities, followed by two rounds of preparative reverse-phase high-performance liquid chromatography (HPLC) (Experimental Procedures). Examination of the purified erythrochelin using MS revealed the presence of the molecular ions for both iron-free *apo*-erythrochelin (*m/z* 604.3) and for iron-bound erythrochelin (*m/z* 657.2), and indicated that a 1:1 complex is formed between the tris(hydroxamate) erythrochelin and Fe(III) under these conditions. The identity of each peak was confirmed by high-resolution MS both of metal-free erythrochelin (calc. 604.2937, found 604.2942) and of the iron-bound form (calc. 657.2052, found 657.2053).

The structure of *apo*-erythrochelin **4** (Figure 2A) was determined by one- and two-dimensional NMR spectroscopy. The 1D- ^1H and ^{13}C NMR spectra of **4** were fully assigned (Experimental Procedures) and supported a tetrapeptide structure comprising one serine and three modified ornithine residues (Orn1-Ser-Orn2-Orn3) (α-*N*-acetyl-δ-*N*-acetyl-δ-*N*-hydroxyornithine-serine-δ-*N*-hydroxyornithine-δ-*N*-acetyl-δ-*N*-hydroxyornithine), including the likely presence of a 2,5-diketopiperazine ring (suggested by the very small scalar coupling between the amide protons of the Orn 2 and Orn 3 residues with their respective α-protons in dimethyl sulfoxide [DMSO]). Long-range carbon-carbon (HMBC, Figure 2A) and proton-proton (NOESY/ROESY) correlations (data not shown) were consistent with structure **4,** but the ultimate structural proof came from the preparation of the Gallium (III)-erythrochelin complex **5** and its NMR analysis (Figure 2B and Experimental Procedures; see Figures S1B and S1C available online). For **5** an upfield shift of the serine and of the two δ-*N*-acetyl-δ-*N*-hydroxyornithine (Orn 1 and Orn 3) carbonyls was observed in the ^{13}C spectrum, indicating coordination to Gallium. Also ROESY/ NOESY correlations between the *N*-methylene protons of Orn2 and the protons (α and β) of the serine were observed (Figure 2B; Figure S1C). Analogous correlations have been previously reported for the threonine of the Gallium (III)-coelichelin complex and its adjacent δ-*N*-hydroxyornithine (Lautru et al., 2005). This confirmed the isopeptide linkage between the serine of erythrochelin and its adjacent δ-*N*-hydroxyornithine (Orn 2) and suggested for the serine the same (D) configuration previously established for the threonine in coelichelin.

The structure of erythrochelin as represented in Figure 2A is chemically identical to the known actinomycete siderophore foroxymithine **3** (Umezawa et al., 1985) except that the two δ-*N*-formyl groups in **3** are replaced by two δ-*N*-acetyl groups in erythrochelin. The stereochemical configuration of

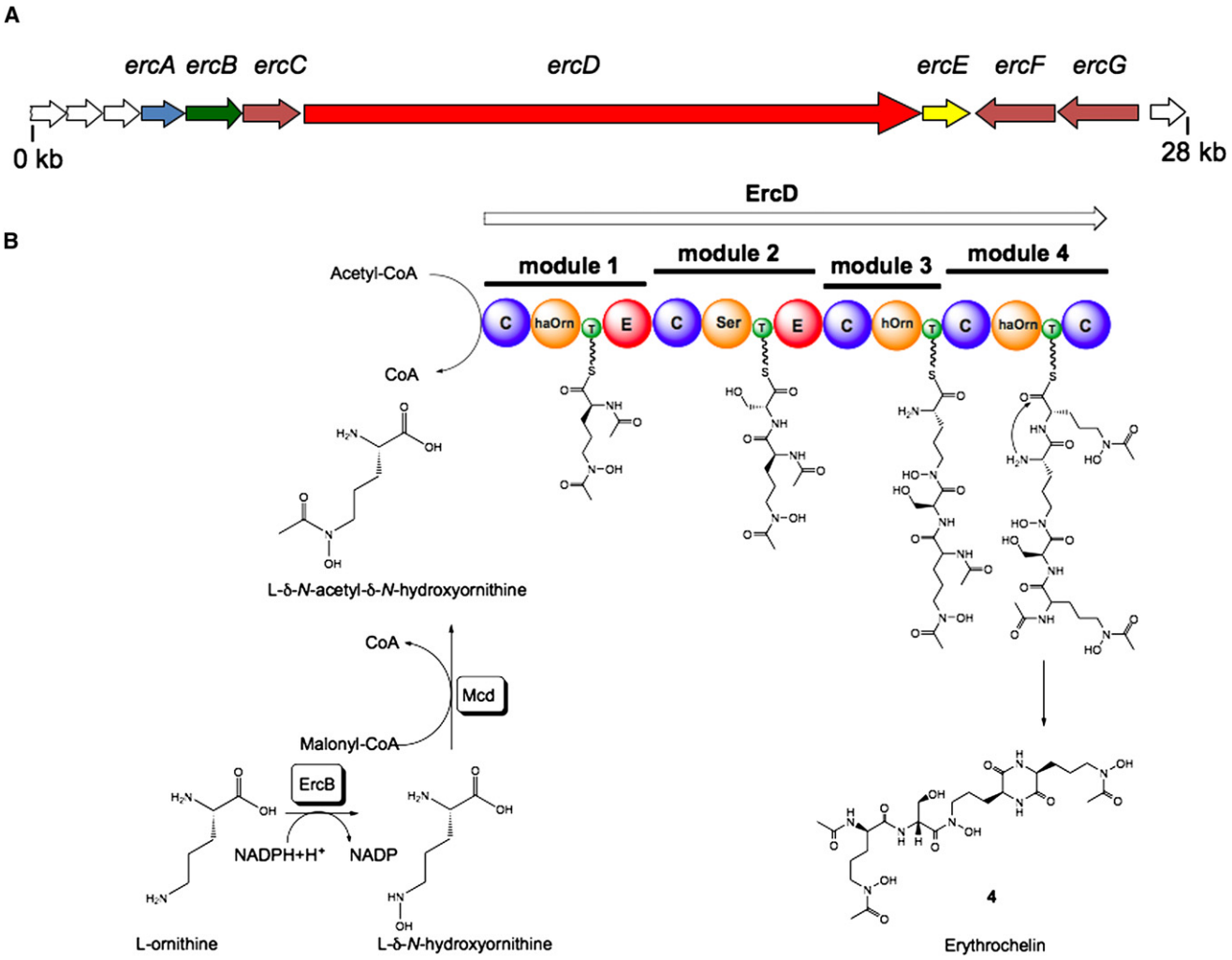

Figure 3. The Erythrochelin Biosynthetic Gene Cluster (*erc*)

(A) The gene arrangement of the *nrps5* (*erc*) cluster of *S. erythraea*. ErcA (SACE_3032), LysR regulator; ErcB (SACE_3033), δ-*N*-ornithine monooxygenase; ErcC (SACE_3034), ferric-siderophore lipoprotein receptor; ErcD (SACE_3035), nonribosomal peptide synthetase; ErcE (SACE_3036), MbtH-like protein; ErcF (SACE_3037) and ErcG (SACE_3038), ABC-type permease.

(B) The proposed mechanism of erythrochelin biosynthesis. Mcd, GCN5-like acetyltransferase; C, condensation domain; A, adenylation domain, T, peptidylcartrier protein (PCP) domain, E, epimerase domain. For further details see the text.

foroxymithine has not been reported, while the configuration shown for erythrochelin in Figure 2A is based on biosynthetic considerations (see below).

Bioinformatic Analysis of *S. erythraea* NRPS Clusters Identifies *nrps5* as a Candidate Cluster to Encode Erythrochelin Biosynthesis

Previous analysis of the *S. erythraea* genome sequence (Oliynyk et al., 2007) identified *nrps3* and *nrps5* as the gene clusters most likely to direct the biosynthesis of siderophores, based on the presence of genes typical of authentic NRPS-dependent siderophore gene clusters. The arrangement of the *nrps5* (*erc*) gene cluster is shown in Figure 3A. The NRPS multienzyme encoded by *ercD* (SACE_3035) contains four modules, each of which contains the essential condensation (C), adenylation (A), and peptidyl carrier protein (PCP) domains (Figure 3B). Modules 1 and 2 also each contain an epimerization (E) domain, indicating that the initially-activated L-amino acids in these modules are converted into the D-isomers during chain synthesis. The amino acid building blocks activated by NRPS ErcD were inferred by examining A domain sequences and in particular the identity of the specificity-conferring residues in each A domain was compared to adenylation domains of known specificity (Stachelhaus et al., 1999; Challis et al., 2000; Rausch et al., 2005) (Table 1).

Consistent with the NMR evidence for the presence of Ser and δ-*N*-hydroxyornithine (hOrn) residues in erythrochelin, analysis of domains A2 and A3 of ErcD (Table 1) (Oliynyk et al., 2007) showed that domain A2 has specificity-conferring residues identical to those of an L-serine-activating A domain of the enterobactin biosynthetic gene cluster of *Escherichia coli* (Gehring et al., 1998) while those of domain A3 are identical to those of domain A3 of the coelichelin NRPS, which is known to activate hOrn (Lautru et al., 2005). Examination of the sequences of domains A1 and A4 of ErcD (Table 1) showed that A1 and A4

Table 1. Comparison of Specificity-Determining Amino Acid Residues in A Domains of the Erythrochelin NRPS with A Domains of Known Specificity

A Domain	Active-Site Residues	Substrate	Product
A1	D V W A L G A V D M E A D G A V	L-Citrulline	Enduracidin
A2	D V W H F S L V D V W H F S L V	L-Serine	Enterobactin
A3	D M E N L G L I D M E N L G L I	L-hOrnithine	Coelichelin
A4	D V F A L G A V D M E A D G A V	L-Citrulline	Enduracidin

are likely to activate the same amino acid, and, as judged by comparison to the sequence of the coelichelin A1 domain (data not shown), this amino acid is very unlikely to be L-δ-*N*-formyl-δ-*N*-hydroxyornithine. NRPS genes known to govern incorporation of L-δ-*N*-acetyl-δ-*N*-hydroxyornithine (haOrn) have not been previously sequenced from bacteria, but are known in fungal systems (Schwecke et al., 2006). Unfortunately, comparison of the A domain sequences did not reveal any informative similarities in the specificity-conferring residues. The closest match to published database sequences of both A1 and A4 is with EndB-m7 of the enduracidin biosynthetic gene cluster of *Streptomyces fungicidus* (Yin and Zabriskie, 2006), which activates the structurally related amino acid citrulline.

The C domain at the N terminus of ErcD is proposed to catalyze the condensation of an acetyl moiety (derived from acetyl-CoA) with the activated δ-*N*-acetyl-δ-*N*-hydroxyornithinyl-PCP in module 1. For other "starter" C domains, it has been demonstrated that in phylogenetic reconstructions these domains can be identified and discriminated from other C domains (Rausch et al., 2007). However, when we analyzed the ercD N-terminal C domain in this way it did not group with the previously identified starter domains, many of which activate quite structurally different aryl and acyl groups. In the acylation of the N-terminal amino acid seen in the biosynthesis of surfactin (Steller et al., 2004), an external (type II) thioesterase, SrfD, catalyzes the transfer of β-hydroxymyristoyl group from CoA to SrfA before condensation with the Glu substrate tethered to the module 1 PCP of SrfA (Steller et al., 2004). It is possible that an analogous thioesterase acts here, and it cannot be ruled out that the acyl donor is malonyl-CoA rather than acetyl-CoA. Another possibility is that the donor is an acyl-ACP, which must be encoded, together with the putative thioesterase, elsewhere on the chromosome. At the C terminus of ErcD, instead of a conventional thioesterase (TE) domain (Kohli and Walsh, 2003), a C domain is present which we propose catalyzes the cyclization of the tetrapeptide to form the 2,5-diketopiperazine. The fungal NRPS that governs the biosynthesis of the diketopiperazine (DKP) core of gliotoxin has been characterized and it also lacks a C-terminal TE. In its place there is a pendant PCP-C di-domain that may be involved in cyclization (Balibar and Walsh, 2006). The ErcD and gliotoxin C-terminal C domains do not show particularly close mutual sequence similarity, and comparison of the ErcD C-terminal C domain active site sequence with that of other C domains did not reveal informative overall differences (Rausch et al., 2007). However, comparison with the core conserved motifs of C domains involved in chain extension (Konz and Marahiel, 1999) showed that the C3 (active site) core consensus sequence in the C-terminal C domain of ErcD is MHYLGIDEWS, instead of the consensus C3 sequence MHHxISDG(WV)S, which might reflect its activity as a cyclase. Alternatively, this C domain might be inactive, and the cyclization (and release) might take place by spontaneous diketopiperazine formation. Further work will be required to distinguish between these alternatives. The upstream edge of the *nrps5* cluster, now renamed *erc*, appears to be defined by *ercA* (SACE_3032), predicted to encode a regulatory protein of the LysR family. The gene product of *ercB* (SACE_3033) is predicted to have 69% sequence identity with the *N*-δ-ornithine hydroxylase of the *S. coelicolor* coelichelin cluster (CchB) (Barona-Gómez et al., 2006), and ErcB is proposed to fulfill the same role in erythrochelin biosynthesis. Other genes for coelichelin biosynthesis also have evident counterparts in the *erc* cluster: for example, the gene product of *ercC* (SACE_3034) has a sequence that is 37% identical to CchF, which has been proposed to encode a membrane-anchored ferric-siderophore lipoprotein receptor required for the uptake of ferric-siderophore complexes (Kim et al., 2005). The coelichelin cluster also contains three other genes (*cchCDE*), which encode permease and ATPase components of an ABC-type importer of the ferric-siderophore complex (Barona-Gómez et al., 2006). In *S. erythraea*, three genes that closely resemble *cchCDE* are found elsewhere in the genome (SACE_4011-4013) and may fulfill the same role for erythrochelin.

The downstream edge of the *erc* cluster appears to be defined by *ercF* (SACE_3037) and *ercG* (SACE_3038), whose gene products show significant sequence similarity respectively to CchG and CchI, ATP-dependent permeases involved in export of the siderophore. Finally, *ercE* (SACE_3036) encodes a small protein of the so-called MbtH family, highly conserved in NRPS clusters but of unknown function (Yeats et al., 2003). It has been shown that when the MbtH gene of an NRPS-dependent cluster is specifically deleted, the MbtH gene of a different cluster can take over this role (Barry and Challis, 2009). The genes immediately flanking *ercA-ercG* cannot yet be definitely ruled out of a role in erythrochelin biosynthesis, but their predicted functions (SACE_3031 hypothetical protein; SACE_3030 adenylate kinase; SACE_3039_hypothetical regulatory protein; SACE_3040 carnitine dehydratase) make it hard to suggest plausible roles for them in erythrochelin biosynthesis.

Specific Deletion of the NRPS Gene *ercD* Abolishes Erythrochelin Biosynthesis in *S. erythraea*

Further evidence that the *erc* gene cluster governs biosynthesis of erythrochelin was sought by creating a mutant, starting from *S. erythraea* JC2, in which the open reading frame of *ercD* was specifically disrupted using the Redirect methodology (Gust et al., 2003), which is based on RedET-mediated recombination (Zhang et al., 1998). The mutant was verified by polymerase chain reaction (PCR) and sequence analysis (Experimental Procedures). In parallel, a further two mutants were made starting from JC2: one mutant was made bearing an analogous disruption (removal of an NRPS open reading frame, replacement with an antibiotic resistance cassette) in the *nrps3* gene cluster, which from sequence comparisons is also predicted to

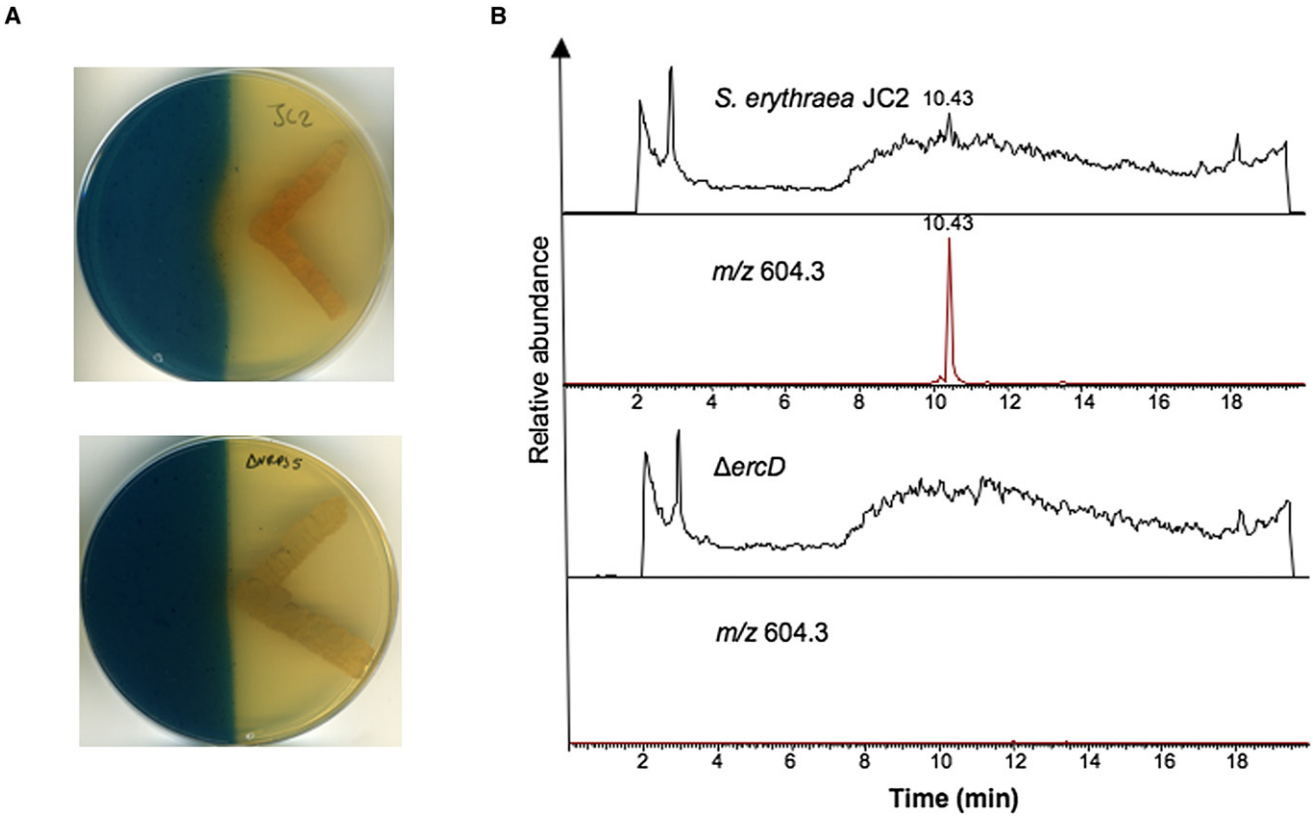

Figure 4. Siderophore Activity of the *S. erythraea* ΔercD Strain

(A) CAS agar assay for the presence of a diffusible hydroxamate siderophore, contrasting the parent strain, *S. erythraea* JC2 (top) with the JC2 ΔercD strain (bottom).

(B) Analysis of the agar medium by LC-MS, showing that in the JC2 ΔercD strain erythrochelin biosynthesis has been abolished. See also Figure S2 in the Supplemental Information.

govern biosynthesis of a siderophore, and which transcriptional analysis (Peano et al., 2007) suggests may be expressed at the same time as *erc*. A second mutant was designed to contain a disruption in the gene cluster *nrps1*, in which an NRPS-encoding gene contains an apparently-inactivating frameshift (Oliynyk et al., 2007).

Each mutant was cultivated in an iron-depleted agar medium under the same conditions as both the *ery*$^-$ JC2 strain of *S. erythraea* from which they were derived, and the wild-type NRRL2338 strain, and extracts of the agar medium were checked using liquid chromatography (LC) MS for the presence of the erythrochelin siderophore. As shown in Figure 4A, when compared with the JC2 strain (top), the ΔercD mutant (bottom) did not produce a diffusible hydroxamate siderophore, as judged by its ability to decolorize chrome azurol S (CAS) (Schwyn and Neilands, 1987; Milagres et al., 1999). Extraction and MS analysis of the agar medium from around the *S. erythraea* strains showed that erythrochelin biosynthesis was abolished in the ΔercD mutant, as judged by the lack of the *m/z* 604.3 $[M+H]^+$ peak. All the other strains tested (NRRL2338, JC2, nrps1, nrps3) did produce erythrochelin (data not shown). Further, the ΔercD mutant did not show the antibiotic activity of the JC2 strain against *Bacillus subtilis* or *Micrococcus luteus* (Figure S2).

The Gene Encoding the δ-*N*-L-acetyltransferase Required for Erythrochelin Biosynthesis (*mcd*) Is Located in the NRPS-Containing Cluster *nrps1*

The formyltransferase CchA involved in coelichelin biosynthesis in *S. coelicolor* is an integral component of the biosynthetic cluster (Lautru et al., 2005), so it was surprising that the *erc* gene cluster did not contain a gene encoding the δ-*N*-hydroxy-L-ornithine acetyltransferase required for erythrochelin biosynthesis. A BLAST search was therefore made of the complete genome sequence of *S. erythraea* to identify candidate genes that might encode an *N*-acetyltransferase activity. As query sequences, we used putative acetyl-CoA: *N*-acetyltransferases found in the biosynthetic gene clusters to bacterial siderophores produced by NRPS-independent routes (Challis, 2005). All of these enzymes when used in BLAST searches show modest but significant sequence similarity to *N*-acetyltransferases involved in diverse cellular processes, including modification of aminoglycoside antibiotics and of histone proteins in eukaryotes (Dyda et al., 2000). A founding member of this family of proteins, IucB, is required for the production of aerobactin in *E. coli* (De Lorenzo and Neilands, 1986; Martínez et al., 1994).

When the *S. erythraea* genome was screened using the IucB protein sequence, the only significant hit (out of nearly 8000

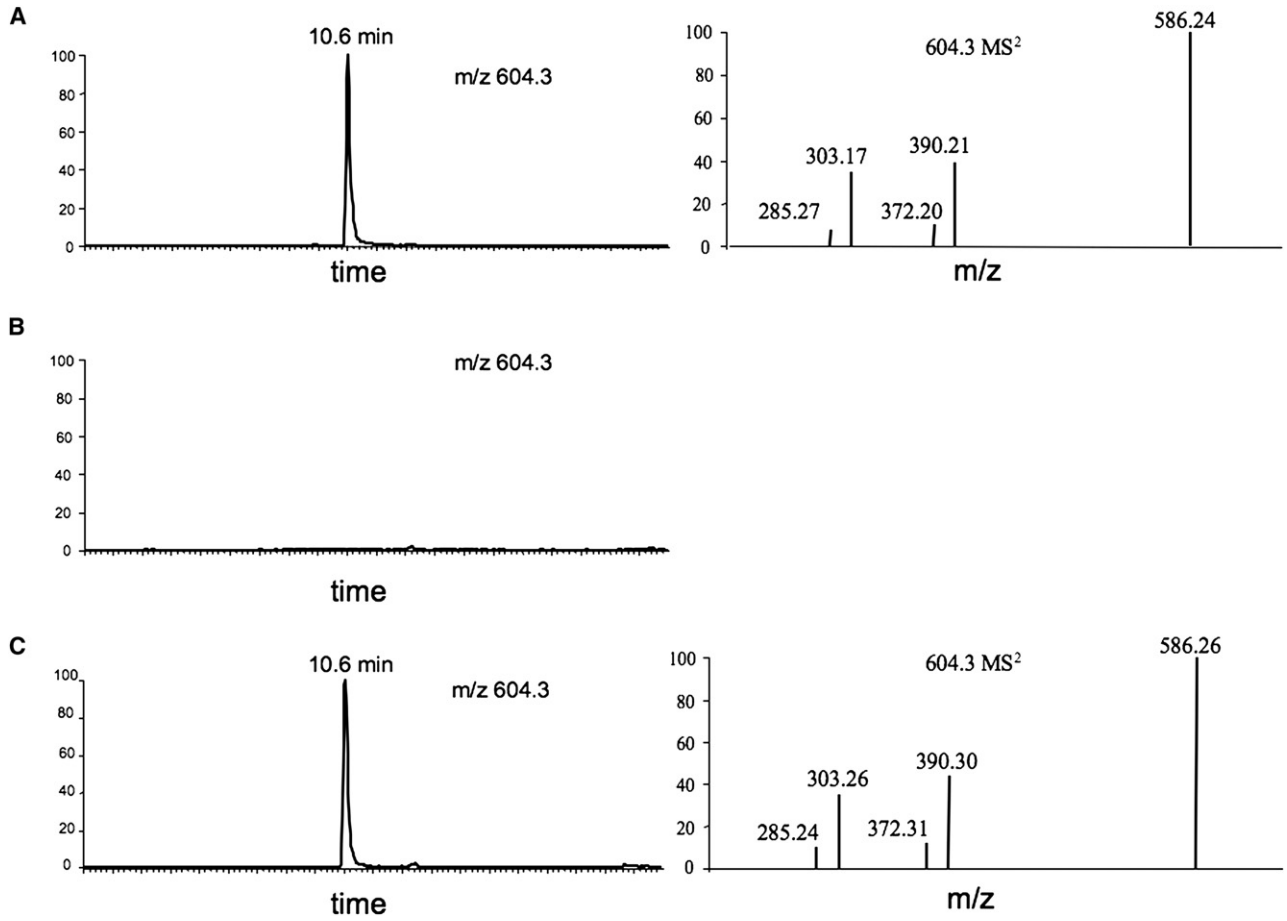

Figure 5. Loss of Erythrochelin Production in a Δ*mcd* Mutant, and Restoration of Production by Added δ-*N*-acetyl δ-*N*-hydroxy-L-ornithine

(A) *S. erythraea* JC2 grown in liquid tap water medium (TWM).

(B) *S. erythraea* JC2 Δmcd mutant grown in TWM.

(C) *S. erythraea* JC2 Δmcd mutant grown in liquid TWM supplemented with 5 mM δ-*N*-acetyl δ-*N*-hydroxy-L-ornithine. Erythrochelin was detected in LC-MS by monitoring its molecular ion $(M+H)^+$ at *m/z* 604.3. See also Figure S3 in the Supplemental Information.

open reading frames) was found to SACE_1304 (33% identity, 49% similarity, expect = $2e^{-12}$). Surprisingly, this was a gene already allocated to the NRPS-containing gene cluster *nrps1*, located nearly 2 Mbp away from the *erc* cluster on the chromosome. The resemblance of SACE_1304 to *N*-acetyltransferases had previously been noted (Oliynyk et al., 2007), but it had also been previously characterized and named as *eryM* or *mcd*, and its gene product had been shown to catalyze the biotin-independent decarboxylation of malonyl-CoA (Hunaiti and Kolattukudy, 1984,1994). The product of the *nrps1* cluster in *S. erythraea* is not known, and an evident frameshift in one of the NRPS genes of this cluster had suggested (Oliynyk et al., 2007) that it might be nonfunctional.

The sequence of the C-terminal domain of Mcd (residues 243–417) strongly resembles that of the GCN5-like acetyltransferase (GNAT) domain in the loading module of certain type I polyketide synthases (PKSs) (Piel et al., 2004; Partida-Martinez and Hertweck, 2007; Gu et al., 2007). Biochemical and structural analysis of the GNAT domain from the loading module of the curacin PKS has demonstrated that the domain is bifunctional, catalyzing both the decarboxylation of malonyl-CoA to acetyl-CoA and subsequent acetyl transfer to the 4′-phosphopantetheinyl prosthetic group of an adjacent ACP domain (Gu et al., 2007). The N-terminal domain of Mcd (residues 1–242) bears no significant sequence similarity to any protein in the public databases.

We hypothesized that Mcd might catalyze both the decarboxylation of malonyl-CoA to acetyl-CoA and also subsequent acetyl transfer from acetyl-CoA to the δ-amino group of δ-*N*-hydroxy-L-ornithine, to provide the haOrn building block for erythrochelin biosynthesis. The *mcd* gene was specifically disrupted in wild-type *S. erythraea* NRRL2338 using the Redirect method (Gust et al., 2003), as described in Experimental Procedures, and the resulting mutant was cultured in tap water medium (TWM) (Rowe et al., 1998). As shown in Figure 5A, the wild-type strain produces erythrochelin under these conditions. However (Figure 5B) the Δmcd strain produces no detectable erythrochelin, which is consistent with an essential role for the *mcd* gene product in biosynthesis of this siderophore (the Δmcd strain also shows no ability to decolorize chrome azurol S [CAS]) (Figure S3).

Repeated attempts were made to complement the *mcd* mutation by a copy of the gene introduced in *trans*, and thereby to restore erythrochelin production. When these proved unsuccessful, for reasons that remain unclear, we turned to an alternative approach to confirm that specific loss of *mcd* was indeed responsible for the loss of siderophore production. The presumed product of the Mcd-catalyzed reaction, δ-*N*-acetyl-δ-*N*-hydroxy-L-ornithine, was synthesized by a published procedure (Custot et al., 1996). The JC2 and Δmcd strains were inoculated from seed cultures and allowed to grow in TWM medium for 72 hr, at which time the wild-type strain would be expected to start to produce erythrochelin (Peano et al., 2007). The Δmcd strain was then supplemented with δ-*N*-acetyl-δ-*N*-hydroxy-L-ornithine, and fermentations were allowed to proceed for a further 72 hr. Figure 5C shows that supplementation with 2 mM δ-*N*-acetyl-δ-*N*-hydroxy-L-ornithine fully restored erythrochelin production under these conditions. When supplementation was omitted, no erythrochelin was produced (Figure 5B). Moreover, supplementation of the Δmcd strain with 2 mM δ-*N*-hydroxy-L-ornithine failed to restore erythrochelin production (data not shown).

DISCUSSION

Siderophore Biosynthesis in *S. erythraea*

Siderophore biosynthesis in *S. erythraea* has not been previously studied, apart from a single report of an uncharacterized hydroxamate as a putative siderophore (Oliveira et al., 2006). It now appears that the latter report very likely refers to erythrochelin and so the name erythrobactin (Oliveira et al., 2006) should be dropped as a separate designation (J. Ward, personal communication). The genome sequence of *S. erythraea* (Oliynyk et al., 2007) has revealed that the gene clusters *nrps3* and *nrps5* are strong candidates to encode an NRPS-dependent pathway to a siderophore. While the present study was in progress, transcriptional profiling of secondary metabolite biosynthesis in *S. erythraea* conducted in the rich medium SCM (Peano et al., 2007), revealed that the *ercBCDE* genes of the *nrps5* cluster (SACE_3033-3036) are coordinately expressed (probes for *ercF* and *ercG* [SACE_3037 and SACE_3038] were absent from the microarray chip). The transcriptional analysis also showed coordinate expression of certain genes in the *nrps3* cluster, and it remains unclear what role if any those gene products play in iron homeostasis. Many micro-organisms do produce structurally different extracellular iron scavengers as well as intracellular molecules for iron sequestration. A caveat to bear in mind is that to qualify as a true siderophore in *S. erythraea* a compound must be demonstrated to be secreted, to bind iron, and for the complex to be taken up by the cell, and only for erythrochelin do we have clear experimental evidence, and then only for the first two steps.

The chance observation of a residual antibiotic activity of *S. erythraea* against Gram-positive bacteria in the absence of erythromycin production has led to purification of a compound active in the CAS assay for hydroxamate iron-chelating compounds. Spectroscopic analysis using MS and NMR has revealed it to be a tetrapeptide tris(hydroxamate) **4**, which we have dubbed erythrochelin. Its chemical structure is almost identical to that of the authentic hydroxamate chelator foroxymithine **3**, which has found clinical application in cancer therapy (Imoto et al., 1987) and as an inhibitor of angiotensin 1 converting enzyme (Aoyagi et al., 1985). Specific disruption of the NRPS-encoding gene in the *nrps5* cluster using the Redirect procedure (Gust et al., 2003) totally abolished both erythrochelin production and CAS reactivity (Figure 4), whereas similar disruption of an NRPS-encoding gene in *nrps3* had little or no effect. This result unequivocally points to erythrochelin as the product of the orphan *nrps5* cluster (now *erc*), and suggests that no other hydroxamate siderophore is produced in significant amounts under the conditions used.

In other actinomycetes NRPS-dependent siderophore gene clusters typically contain iron-regulated promoters, and a consensus palindromic nucleotide sequence has been deduced for these "iron boxes," which are thought to bind specific repressor proteins when iron is present (Flores and Martin, 2004). However, no such iron box consensus sequence could be detected in intergenic regions in the *erc* cluster. Whatever the mechanism of iron-mediated regulation turns out to be, it is clear from the present study (and from the work of Peano et al., 2007) that erythrochelin is produced at significant levels in fermentation media that contain iron. Erythrochelin exerts an antibiotic effect on agar plates against *Bacillus* and *Micrococcus* spp. and we assume that erythrochelin exerts this activity by depletion of iron from the medium, but a more direct effect on the target bacteria cannot be ruled out.

The Erythrochelin Synthetase Is an Orthodox Modular NRPS

Linkage of erythrochelin biosynthesis to the gene cluster *erc* led directly to the biosynthetic scheme proposed in Figure 3B: peptide synthesis is initiated by α-acetylation/epimerization of L-δ-*N*-acetyl-δ-*N*-hydroxyornithine (haOrn) within the first (N-terminal) module of the tetramodular ErcD NRPS. Condensation with L-serine, which is activated and epimerized within module 2, is followed by formation of an isopeptide bond between the Ac-D-haOrn-D-Ser (bound in thioester linkage to PCP2) and the δ-amino group of an L-δ-*N*-hydroxyornithine (hOrn) amino acid residue activated in module 3. Further condensation with L-δ-*N*-acetyl-δ-*N*-hydroxyornithine (haOrn), bound and activated in module 4, produces a tetrapeptide via an orthodox modular mechanism. This is in sharp contrast to the unorthodox mechanism, previously uncovered by genome mining, for biosynthesis of the hydroxamate siderophores fuscachelin **1** (Dimise et al., 2008), and coelichelin **2** (Lautru et al., 2005), which in each case involves skipping and re-use of NRPS modules during chain elongation (Figure 6). The availability of such closely-related NRPS systems acting by such different chain extension mechanisms offers a fascinating opportunity to study the factors involved. Chain termination and release of erythrochelin is proposed to involve cyclization to the diketopiperazine, catalyzed by the C-terminal C domain (Figure 3B). C domains have been previously implicated in the analogous off-loading of nonribosomal peptides to amine acceptors in both vibriobactin and anguibactin biosynthesis (Crosa and Walsh, 2002). Sequence comparisons with these domains, and with other "TE-like" C domains from fungi, did not reveal any obvious common features that distinguish them as a group. However, the active site motif of the ErcD C-terminal C domain does show a different motif at its active site (HYGLIDE) compared to C domains involved in chain extension.

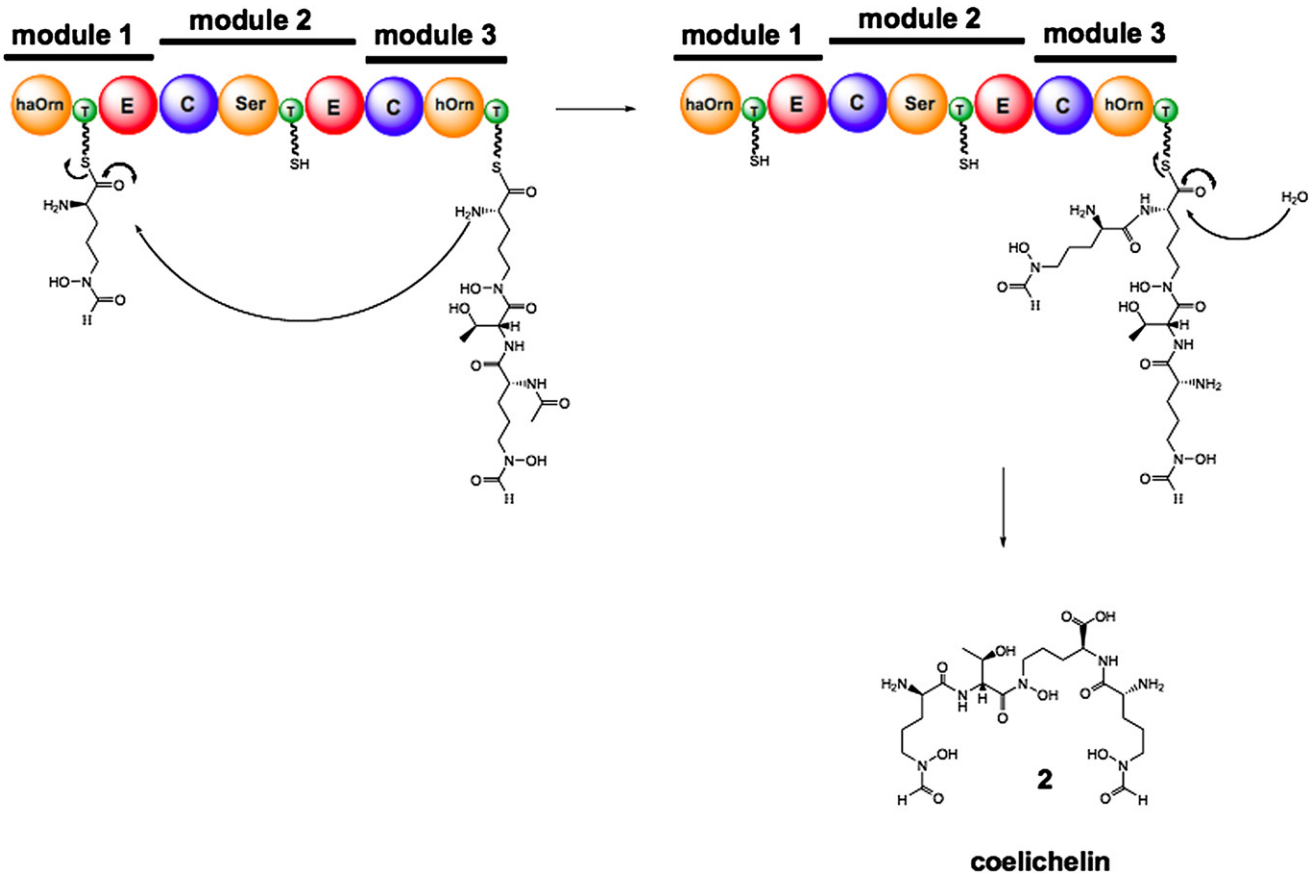

Figure 6. The Proposed Mechanism of Assembly of Coelicoelin

The trimodular NRPS is proposed to synthesize the tetrapeptide siderophore **2** (rather than the predicted tripeptide) by re-use of module 1 to load an additional δ-*N*-formyl-δ-N-hydroxyl-L-ornithine residue and coupling of this to the tripeptide attached in module 3 (Lautru et al., 2008). This is in contrast to the orthodox assembly pattern proposed here for the tetramodular erythrochelin NRPS (Figure 3B).

Erythrochelin is predicted on biosynthetic grounds to have the configuration shown in Figure 2 in which the four amino acids have D-, D-, L- and L- configuration respectively. This contrasts with the all L- configuration reported for foroxymithine **3** (Figure 1) (Umezawa et al., 1985; Dolence and Miller, 1991). Our NMR analysis (Figure 2B and Experimental Procedures; Figures S1B and S1C) of the 1:1 gallium: erythrochelin complex is consistent with the Ser residue in erythrochelin having the D- configuration, but further work will be required to confirm the full stereostructure. The NMR analysis of the gallium complex also revealed the existence of multiple sets of signals (Experimental Procedures; Figure S1B), which may indicate slow rotation around amide bonds (as previously suggested for synthetic precursors to foroximithine, Dolence and Miller, 1991) or alternative arrangements of the (tris)hydroxamate ligands around the metal ion (Knof and von Zelewsky, 1999).

A δ-*N*-acetyltransferase Activity Essential for Erythrochelin Biosynthesis Is Encoded by the Gene *mcd* Located in a Remote *nrps* Cluster

Crosstalk between metabolic pathways in actinomycete bacteria is a well-known phenomenon. This may involve the sharing of one or more enzymes by two different pathways, as for example the malonyl-CoA transferase (MAT) of *S. coelicolor* fatty acid synthase, which is also proposed to function in the polyketide synthase (PKS) pathway that leads to the isochromanequinone pigment actinorhodin (Revill et al., 1995; see also Summers et al., 1995). Similarly, the dTDP-L-rhamnose biosynthetic enzymes of *Saccharopolyspora spinosa*, which provide an essential sugar moiety for the insecticidal polyketide spinosyn A, are proposed to be required also for production of the rhamnolipids of the bacterial cell wall (Madduri et al., 2001). Other enzymes potentially involved in more than one pathway are the auxiliary transferase enzymes that attach the essential 4′-phosphopantetheine prosthetic group to acyl carrier proteins or domains (ACPs) in FAS and PKS, and to peptide carrier proteins or domains in nonribosomal peptide biosynthesis. Here, the specificity of individual enzymes is less clear-cut. Some of these are capable of activating a wide range of ACP and PCP substrates, for example the Sfp phosphopantetheinyltransferase associated with surfactin biosynthesis in *Bacillus subtilis*. Others are completely specific for a single substrate, such as the SePptII phosphopantetheinyltransferase in *S. erythraea*, which assures prosthetic group attachment to the erythromycin PKS (Weissman et al., 2004).

Crosstalk has also been used to refer to a situation, frequent in actinomycetes, where multiple highly similar enzymes carry out

the same catalytic function in different pathways. Deletion of the gene for one of these enzymes may not block the relevant pathway, because one or more of the counterpart enzymes from other pathways may take over the missing function. For example, the *erc* cluster does not contain genes for a discrete (type II) thioesterase (TE) enzyme. Such TEs are a common feature of NRPS clusters, including the *nrps2*, *nrps3,* and *nrps7* clusters of *S. erythraea* (Oliynyk et al., 2007), and they have been ascribed a generic role in speeding up the removal of aberrantly acylated active sites on the NRPS (Schwarzer et al., 2002). It may be that the *erc* cluster relies upon one of these TE enzymes fulfilling such a function for ErcD. Alternatively, the *erc* TE may reside unrecognized elsewhere on the chromosome. As mentioned in the Results section, an acyltransferase and ACP encoded elsewhere might conceivably function in the N-terminal acylation step. Likewise, the *nrps3*, *erc* and *nrps7* clusters of *S. erythraea* each contain an MbtH-like gene, encoding a small, highly conserved protein of unknown function found in many other (but not all) NRPS biosynthetic gene clusters. When an MbtH-like gene was deleted from the NRPS-dependent cluster in *Amycolatopsis balhimycina* for the biosynthesis of the glycopeptide balhimycin, the resulting mutant continued to produce the antibiotic at wild-type levels, hinting at a possible functional crosstalk between MtbH-like genes (Stegmann et al., 2006). This has been directly confirmed in *S. coelicolor* by showing that when either one of the MtbH-like genes *cdaX* or *cchX* was deleted the respective pathway continued to function, whereas in a double cdaX$^-$ cchX$^-$ mutant both NRPS-dependent pathways were blocked (Lautru et al., 2007). Fungal examples of this conventional crosstalk have also been described: for example, the bassaniolide cluster relies on an enzyme involved in D-hydroxyisovalerate biosynthesis that is encoded in the beauvericin cluster and essential for production of both metabolites (Xu et al., 2008, 2009).

Here, we have shown that a gene encoding a δ-*N*-acetyltransferase activity (*mcd*) essential for erythrochelin biosynthesis is not located in the *erc* gene cluster. Surprisingly, it has been traced to the apparently defunct *nrps1* cluster, separated by a distance of nearly 2 Mbp from the *erc* gene cluster. This is, to our knowledge, the first example to be discovered of such crosstalk between remote NRPS-containing gene clusters as an *essential* feature of the biosynthesis of a single nonribosomal peptide, rather than opportunistic crosstalk by a functionally similar protein that is only revealed by mutation (Stegmann et al., 2006; Lautru et al., 2007). The *nrps1* cluster has an obvious frameshift in the gene for NRPS1 (Oliynyk et al., 2007). It will be interesting to see whether other examples of such essential crosstalk uncovered in future are also associated with clusters in which a key gene is inactivated by a local mutation.

The attempted complementation in *trans* of the Δmcd mutant, with a copy of the *mcd* gene cloned under the control of the constitutive *ermE** promoter, gave a few, poorly growing colonies that did not produce erythrochelin (data not shown). However, erythrochelin production was fully restored to the Δmcd mutant by the supplementation of the medium with chemically synthesized L-δ-*N*-acetyl-δ-*N*-hydroxyornithine (but not with synthetic L-δ-*N*-hydroxyornithine). These results clearly show that the loss of erythrochelin production in the Δmcd mutant is indeed due to the specific ablation of the *mcd* gene and not to an adventitious secondary mutation. Specifically, a polar effect on the downstream NRPS gene within the *nrps1* gene cluster can be excluded, because the JC2 Δnrps1 mutant produces erythrochelin at the same level as the JC2 parent strain (data not shown). It remains unclear why the attempts at genetic complementation failed, but it is possible that constitutive expression of *mcd* in *trans* might have interfered with other cellular processes by inappropriate acetyl transfer to other metabolites or macromolecules. The successful complementation with synthetic δ-*N*-acetyl-δ-*N*-hydroxy-L-ornithine also reveals the likely timing of the modification of the side chain of L-ornithine. It is fully consistent with a mechanistic scheme in which the flavin-dependent mono-oxygenase ErcB carries out the δ-*N*-hydroxylation of L-ornithine, which is then acetylated by Mcd, so that the two haOrn residues of erythrochelin are formed before their incorporation into the peptide chain (Figure 3B). We have meanwhile expressed Mcd in *E. coli* (Hsieh and Kolattukudy, 1994) and have confirmed that it catalyzes the formation of δ-*N*-acetyl-δ-*N*-hydroxy-L-ornithine from δ-*N*-hydroxy-L-ornithine, using either acetyl-CoA or malonyl-CoA as an acyl donor (Kenning, M., M.T., P.F.L., unpublished data). A similar mechanism has been proposed for the production of haOrn residues both in fungal hydroxamate siderophores (Haas, 2003) and in coelichelin biosynthesis (Pohlmann and Marahiel, 2008; Challis, 2008).

SIGNIFICANCE

Actinomycete genomes encode large numbers of orphan gene clusters encoding unknown secondary metabolites, representing a significant pool of untapped chemical diversity. In this study we describe the isolation and structure determination of a previously unidentified bioactive iron-chelating peptide from the erythromycin-producing strain of *Saccharopolyspora erythraea*, which we have called erythrochelin. Intriguingly, erythrochelin is readily detected in media that are iron replete. Its structure is nearly identical to that of the putative bacterial siderophore foroxymithine, which has found clinical use both as an inhibitor of angiotensin-converting enzyme and in cancer therapy. Assisted by knowledge of the complete genome sequence of *S. erythraea* (Oliynyk et al., 2007), the modular NRPS-containing gene cluster (*nrps5*, *erc*) responsible for erythrochelin biosynthesis has been identified. In contrast to the unusual mechanism recently proposed for other tetrapeptide hydroxamate siderophores, which involves noncanonical use of modules in an NRPS, erythrochelin biosynthesis follows an orthodox colinear mechanism, culminating in release of the chain as a diketopiperazine product. Comparison of these closely related multienzyme systems may offer fresh insights into the factors that determine colinearity. Remarkably, a GCN5-like *N*-acetyltransferase gene (*mcd*) shown here to be required for erythrochelin biosynthesis is located not in the *erc* cluster but in another NRPS-containing cluster (*nrps1*) lying some 2 Mbp distant from the *erc* cluster on the *S. erythraea* genome, an unprecedented example of functional crosstalk between NRPS-dependent biosynthetic pathways. Further examples of such essential crosstalk, as opposed to functional redundancy revealed by mutation, may be uncovered in future, especially in those

actinomycete strains that are prolific in NRPS- and PKS-dependent secondary metabolite biosynthesis.

EXPERIMENTAL PROCEDURES

Strains and Growth Conditions

Saccharopolyspora erythraea NRRL2338 was obtained from the Agricultural Research Service Culture Collection (Peoria, IL). The strain *S. erythraea* JC2 bearing a deletion in almost all of the erythromycin polyketide synthase genes has been previously described (Rowe et al., 1998). General actinomycete cloning procedures were followed as previously reported (Kieser et al., 2000). *E. coli* DH10B (GIBCO BRL) was used as a host for routine cloning procedures (Sambrook et al., 1989). The *E. coli* strains ET12567/pUB307 (Flett et al., 1997) or ET12567/pUZ8002 (Kieser et al., 2000) were used to deliver DNA via conjugation with strains of *S. erythraea*. The integrative expression plasmid pIB139 has been previously described for use in *S. erythraea* (Rowe et al., 2001). *S. erythraea* JC2 was maintained in M79 medium (Kieser et al., 2000) and SM3 medium was used for erythrochelin production. *E. coli* BW25113 (pIJ790), *E. coli* ET12567 (pUZ8002), and the strains housing *S. erythraea* cosmids (Oliynyk et al., 2007) were maintained in 2TY medium supplemented with the appropriate antibiotics. Conjugations were carried out on SFM medium supplemented with 10 mM $MgCl_2$ and the isolates were grown on TWM. Antibiotic concentrations used routinely were: ampicillin 50 mg ml^{-1}, apramycin 50 mg ml^{-1}, chloramphenicol 34 mg ml^{-1}, nalidixic acid 24 mg ml^{-1}, and kanamycin 50 mg ml^{-1}.

Bioassay of *S. erythraea* JC2 and Mutants Derived from it

Each strain was streaked onto nonselective TWM plates and grown for 3 days, after which the plates were overlaid with 2TY soft agar (3 ml) previously inoculated (1:100) with an overnight culture of either *Micrococcus luteus* or *Bacillus subtilis*, and incubated overnight at 37°C.

Detection of Iron Chelators on Chrome Azurol S Agar Plates

All the glassware used to prepare the solutions used in these experiments was soaked in 6M HCl overnight and rinsed with MilliQ water to render it iron-free.

Chrome Azurol S (CAS) agar plates were prepared as previously reported (Schwyn and Neilands, 1987; Milagres et al., 1999). Half of each CAS agar layer was cut out and the gap was filled with TWM agar supplemented with appropriate antibiotics for each strain. *S. erythraea* was plated on the TWM half of the plates in a "V" shape to facilitate visualization of the diffusion of any hydroxamate siderophore (revealed by a color change from blue to orange after incubation at 30°C for 3–10 days).

Purification of Erythrochelin from *S. erythraea* JC2

S. erythraea JC2, maintained on tap water medium (TWM)-agar slants, was used to inoculate 10 ml SM3 liquid culture. The cells were grown for 5 days at 30°C and 250 rpm and then used to inoculate 1 l SM3 medium. The *S. erythraea* JC2 was grown for 5 days in SM3 medium at 30°C and 250 rpm, the broth was clarified by centrifugation at 5000 x *g* for 10 min and the supernatant was sequentially passed through Amberchrom CG161 polystyrene divinyl benzene and Amberlite IRA-68 NR2 (acetate-activated form) columns before being concentrated by freeze-drying. The residue was dissolved in methanol (15 ml), filtered, and applied to an Agilent 1200 preparative HPLC-system fitted with a Phenomenex Luna reverse-phase column (10 μm, 250 × 21 mm), and eluted with a linear gradient of water and 95% methanol (both containing 0.1% formic acid) over 25 min at a flow rate of 20 ml min^{-1}. Erythrochelin elution was monitored by UV absorbance at 210 nm and fractions were tested for the presence of the molecular ion *m/z* 604.3. The fractions containing this material were pooled, freeze-dried, and repurified by HPLC under the same conditions.

Analysis of Erythrochelin by Mass Spectrometry

MS analysis of *apo*-erythrochelin **4** and Ga(III)- erythrochelin **5** was performed using an LTQ-FT instrument (Thermo) connected to a microbore HPLC system (Agilent 1200), fitted with a Phenomenex Prodigy ODS(3) column (250 × 2 mm, 5μm), and the following solvent gradient: 0%–40% acetonitrile/0.1% formic acid over 15 min, then 40%–95% acetonitrile/0.1% formic acid over 5 min, at a flow rate of 0.3 ml min^{-1}. The mass spectrometer was operated in positive-ion mode, scanning from 180 to 2000 *m/z*. HPLC-HR-ESI-MS analysis of purified erythrochelins was performed on a Thermo Electron LTQ-Orbitrap. The samples were injected onto a Dionex Acclaim C18 PepMap 100 column (150 mm × 1.0 mm, 3 μm), eluting with a linear gradient of 0% to 100% B in 28 min with a flow rate of 50 μl/min (A: 98% H_2O, 2% acetonitrile, 0.1% formic acid, B: 90% acetonitrile, 10% H_2O, 0.1% formic acid). The mass spectrometer was run in positive ionization mode, scanning from *m/z* 100 to 1800, with the FTMS analyzer resolution set at 60 K.

Preparation of Gallium (III)-Erythrochelin

All the glassware was sequentially treated with 5M KOH, MilliQ water, concentrated HNO_3 and finally rinsed with MilliQ water to remove trace metals. Following a protocol previously reported (Sharman et al., 1995), a mixture of ferri-erythrochelin and *apo*-(iron-free) erythrochelin (15 mg) was dissolved in MilliQ water (25 ml), mixed with a solution of 8-hydroxyquinoline (145 mg) in methanol (25 ml) and stirred overnight at room temperature. The mixture was repeatedly extracted with dichloromethane (5 × 20 ml), the residual methanol was evaporated and the remaining aqueous solution was freeze-dried. The presence of *apo*-erythrochelin was verified by LC-MS. The residue was dissolved in MilliQ water (25 ml) and Gallium (III) sulfate hydrate (Sigma, 15 mg in 0.5 ml of 0.05 M H_2SO_4) was added. After 30 min, at room temperature the pH was adjusted to 7.0 with NaOH and the mixture was freeze-dried. The residue was redissolved in MilliQ water (1 ml) before being purified by preparative HPLC as described for erythrochelin (with the exception of formic acid not present). The 1:1 Gallium: erythrochelin complex eluted at 7.4 min and MS analysis confirmed the presence of the expected molecular ion *m/z* = 670.2 (HR-ESI-MS shown in Figure S1A, calc. 670.1958, found 670.1936).

Structural Analysis of Erythrochelin Using NMR

The NMR spectra of erythrochelin (*apo*- and Ga (III)-complex, approximately 1 mM samples) were measured at 298 K using Bruker Avance 500 and 700 MHz NMR spectrometers equipped with a TCI cryoprobe. ^{1}H, ^{13}C, DEPT, HMQC, DFQ-COSY, TOCSY (varying mixing time from 60 to 200 mS), HMBC, ROESY, and NOESY (1D and 2D, varying mixing times from 0.5 s to 1 s) spectra were acquired. For ^{1}H- and ^{13}C-NMR, the chemical shifts are reported relative to the solvent signal (CD_3OH δ_H 3.34, DMSO δ_H 2.50, CD_3OD δ_C 49.0 and DMSO δ_C 39.4). The ^{1}H and ^{13}C-NMR signals were assigned with the aid of the 2D experiments. For *apo*-erythrochelin **4**: **^{1}H-NMR (500MHz, CD_3OD)**: δ 5.06 (t, *J* = 5.0, 1H, *CH Ser*), 4.44 (t, *J* = 5.0, 1H, *CH Orn1*), 4.02 (t, *J* = 5.0, 1H, *CH*), 4.00 (t, *J* = 5.0, 1H, *CH*), 3.84-3.81 (m, 2H, CH_2OH *Ser*), 3.76-3.66 (m, 2H, NCH_2 *Orn1* and NCH_2 *Orn2/3*), 3.69-3.59 (m, 3H, NCH_2 *Orn2* and *Orn3*), 3.63-3.54 (m, 1H, NCH_2 *Orn1*), 2.11 (s, 6H, δ-NCOCH_3 *Orn1* and *Orn3*), 2.00 (s, 3H, α−NCOCH_3 *Orn1*), 1.90-1.60 (m, 12H, CH_2); **^{13}C-NMR (125 MHz, CD_3OD)**: δ 174.4 (CONH, *Orn1*), 173.9, 173.8 (δ-NCOCH_3,*Orn1* and *Orn3*), 173.4 (α-NCOCH_3, *Orn1*), 171.4 (CONH, *Ser*), 170.4, 170.4 (CONH, *Orn2* and *Orn3*), 62.4 (CH_2OH, *Ser*), 55.7, 55.2 (CH), 54.3 (CH, *Orn1*), 54.0 (CH, *Ser*), 48.9, 48.9 (NCH_2, *Orn2* and *Orn3*), 48.7 (NCH_2, *Orn1*), 32.3, 32.1, 30.2, 24.1, 23.4, 23.1 (CH_2), 22.4 (α−NCOCH_3, *Orn1*), 20.2 (δ-NCOCH_3, *Orn1* and *Orn3*). **^{1}H-NMR (500MHz, DMSO)**: δ 9.82 (b s, 2H, NO*H*), 8.36 (b s, 1H, NO*H*), 8.15 (bs, 1H, N*H*), 8.10 (bs, 1H, N*H*), 8.00 (d, *J* = 8.3, 1H, N*H Orn1*), 7.77 (b d, *J* = 7.5, 1H, N*H Ser*), 4.86-4.82 (m, 1H, *CH Ser*), 4.84 (b t, 1H, *J* = 5.5, 1H, CH_2O*H Ser*), 4.35-4.30 (m, 1H, *CH Orn1*), 3.81 (bs, 2H, *CH Orn2* and *Orn3*), 3.68-3.50 (m, 2H, CH_2OH *Ser*), 3.63-3.37 (m, 6H, NCH_2), 1.97 (s, 6H, δ-NCOCH_3 *Orn1* and *Orn3*), 1.85 (s, 3H, α−NCOCH_3 *Orn1*), 1.70-1.40 (m, 12H, CH_2); **^{13}C-NMR (125 MHz, DMSO)**: δ 171.6 (CONH, *Orn1*), 170.2, 170.2 (δ-NCOCH_3, *Orn1* and *Orn3*), 169.1, 169.1 (α-NCOCH_3 *Orn1* and CONH *Ser),* 167.9, 167.8 (CONH, *Orn2* and *Orn3*), 60.8 (CH_2OH, *Ser*), 53.7, 53.5 (CH), 52.1, 52.1 (CH, *Orn1* and *Ser*), 47.0 (NCH_2, *Orn1*), 46.8, 46.8 (NCH_2,*Orn2* and *Orn3*), 30.2, 30.1, 29.5, 23.1 (CH_2), 22.5 (α−NCOCH_3, *Orn1*), 22.0, 21.8 (CH_2), 20.4 (δ-NCOCH_3, *Orn1* and *Orn3*).

For Ga(III)-erythrochelin **5**, a double set of signals in approximately 1:1 ratio was observed. The relative ^{1}H-NMR integrations for the two-set signals are given.

^{1}H-NMR (700MHz, DMSO): δ 8.38 (d, *J* = 6.0, 1H, N*H Ser*), 8.36 (d, ^{3}J = 6.0, 1H, N*H Ser*), 8.32 (d, *J* = 3.5, 1H, N*H*), 8.24 (d, *J* = 3.5, 1H, N*H*), 8.20 (d, *J* = 3.5, 1H, N*H*), 8.10 (d, *J* = 3.0, 1H, N*H*), 7.81 (d, *J* = 8.0, 1H, N*H Orn1*), 7.76 (d, *J* = 8.0, 1H, N*H Orn1*), 5.09 (b t, *J* = 5.0, 1H, CH_2O*H Ser*), 4.94 (b t, *J* = 5.0, 1H,

CH_2OH *Ser*), 4.74-4.69 (m, 2H, C*H* Ser), 4.55-4.53 (m, 1H, C*H Orn1*), 4.52-4.49 (b m, 1H, C*H Orn1*), 4.16-4.12 (m, 1H, NCH_2 *Orn2*), 3.97-3.89 (m, 3H, NCH_2 *Orn2*), 3.71-3.69 (m, 1H, C*H*), 3.65-3.57 (m, 4H, CH_2OH *Ser* and C*H*), 3.55-3.53 (m, 1H, CH_2OH *Ser*), 3.52-3.49 (m, 1H, CH), 3.48-3.45 (m, 1H), 3.43-3.39 (m, 2H), (proton signals between 3.38 and 3.21 ppm hidden by water peak), 2.17-2.09 (m, 2H), 2.08, 2.07, 2.05, 2.04 (s, 3H, δ-NCOCH_3 *Orn1* and *Orn* 3), 2.03-1.94 (m, 2H), 1.91-1.80 (m, 2H), 1.85, 1.84 (s, 3H, α−NCOCH_3 *Orn1*), 1.79-1.74 (m, 2H), 1.71-1.57 (m, 6H), 1.47-1.33 (m, 5H), 1.31-1.19 (m, 5H); **^{13}C-NMR (125 MHz, DMSO)**, selected data: δ 171.7, 171.2 (CONH, *Orn1*), 169.4, 169.3 (α-NCOCH_3, *Orn1*), 168.3, 168.1, 168.0, 167.6 (CONH, *Orn2* and *Orn3*), 161.5, 161.3 (CONH, *Ser*), 161.2, 160.9, 160.7, 160.7 (δ-NCOCH_3, *Orn1* and *Orn3*), 60.9, 60.0 (CH_2OH, *Ser*), 55.7, 55.7, 55.4, 55.1 (CH, *Orn 2* and *Orn 3*), 51.1, 51.1 (CH, *Orn 1*), 50.7, 50.5 (NCH_2), 50.1 (CH, *Ser*), 49.9, 49.9 (NCH_2), 49.1 (CH, *Ser*), 22.9, 22.8 (α−NCOCH_3, *Orn1*), 17.3, 17.0, 17.0, 16.9 (δ-NCOCH_3, *Orn1* and *Orn3*).

Construction of Mutant Strains Deleted in Specific Genes in the *nrps* Clusters of *S. erythraea* JC2 Using the Redirect Technique

RedET-mediated recombination in *E. coli* was used to exchange target genes, housed in appropriate *S. erythraea* cosmids, with the apramycin (*aac(3)IV*) resistance cassette, described for the Redirect protocol (Gust et al., 2003). The primers used to perform the gene replacement experiments are listed in Table S1 in the Supplemental Information. Optimal results were achieved using highly concentrated PCR products for the transformation of *E. coli* and twice the concentration of apramycin antibiotic recommended. Each deletion cosmid was used to transform competent cells of the methylation-deficient *E. coli* ET12567 (pUZ8002). Glycerol stocks were made of the successful transformants, which were stored at −80°C before being used in conjugation experiments with *S. erythraea*. Single-crossover transformants of *S. erythraea* were selected for apramycin resistance. The loss of the cosmid backbone was facilitated by the removal of kanamycin selection, resulting in Apr^R/Km^S mutant strains. Single Apr^R colonies were restreaked on TWM agar supplemented with apramycin (50 μg ml^{-1}) and nalidixic acid (24 μg ml^{-1}), and then in liquid M79 medium for three times to facilitate the loss of the Km^R cosmid backbone. Finally they were plated out, and single colonies were tested for the required Apr^R/Km^S phenotype by replica plating. The identity of the deletion mutants was verified by PCR analysis using appropriate oligonucleotide primer pairs (NRPS1TF, NRPS1TR, NRPS3TF, NRPS3TR, NRPS5TF, NRPS5TR) (Table S1) and by sequencing.

Complementation of the Δmcd Mutant

The *mcd* gene was amplified by PCR using primers cMCD_F and cMCD_R (Table S1). The thiostrepton-resistance gene *tsr* along with its promoter was amplified from plasmid pYH7 (Sun et al., 2006) using primers ThioCompF and ThioCompR (Table S1). The two genes were cloned sequentially into the integrative plasmid vector pIB139 (Rowe et al., 2001), which was transferred into *S. erythraea* JC2 Δmcd by conjugation using the *E. coli* strain ET12567 (pUZ8002).

For chemical complementation, δ-*N*-acetyl-δ-*N*-hydroxy-L-ornithine and δ-*N*-hydroxy-L-ornithine were synthesized according to published procedures (Hu and Miller, 1994, Custot et al., 1996). The Δmcd strain was inoculated from seed cultures in TWM medium and grown for 72 hr at 30°C. The culture was then supplemented with either δ-*N* -acetyl-δ-*N*-hydroxy-L-ornithine or δ-*N*-hydroxy-L-ornithine (both 2 mM). Control incubations were left without a supplement. Fermentation was continued for a further 48 hr, after which the culture supernatants were analyzed by LC-MS.

SUPPLEMENTAL INFORMATION

Supplemental Information includes three figures and one table and can be found with this article online at doi:10.1016/j.chembiol.2010.01.011.

ACKNOWLEDGMENTS

We thank Mike Kenning, Barrie Wilkinson (Biotica), Greg Challis (Warwick), and Mohamed Marahiel (Marburg) for useful discussions, and for sharing data prior to their publication. We also thank Duncan Howe and Peter Grice (Department of Chemistry, Cambridge) for the NMR data acquisition. This research was supported in part by grant 8/CFB17699 from the Biotechnology and Biological Sciences Research Council (BBSRC) (U.K.) (to P.F.L.); by a PhD studentship funded by Glaxo Group Research (now GSK) (to S.B.), and by a short-term studentship funded by the Nuffield Foundation (to A.S.). M.T. is a Senior Research Fellow supported by the Herchel Smith Fund of the University of Cambridge.

Received: November 10, 2009
Revised: January 14, 2010
Accepted: January 21, 2010
Published: February 25, 2010

REFERENCES

Aoyagi, T., Wada, T., Iinuma, H., Ogawa, K., Kojima, F., Nagal, M., Kuroda, H., Obayashi, A., and Umezawa, H. (1985). Influence of angiotensin-converting enzyme inhibitor, foroxymithine, on dynamic equilibrium around the renin-angiotensin system in vivo. J. Appl. Biochem. *7*, 388–395.

Balibar, C.J., and Walsh, C.T. (2006). GliP, a multimodular nonribosomal peptide synthetase in *Aspergillus fumigatus*, makes the diketopiperazine scaffold of gliotoxin. Biochemistry *45*, 15029–15038.

Banskota, A.H., McAlpine, J.B., Sørensen, D., Ibrahim, A., Aouidate, M., Piraee, M., Alarco, A.-M., Farnet, C.M., and Zazopoulos, E. (2006). Genomic analyses lead to novel secondary metabolites: Part 3. ECO-0501, a novel antibacterial of a new class. J. Antibiot. (Tokyo) *59*, 533–542.

Barona-Gómez, F., Lautru, S., Francou, F.X., Leblond, P., Pernodet, J.L., and Challis, G.L. (2006). Multiple biosynthetic and uptake systems mediate siderophore-dependent iron acquisition in *Streptomyces coelicolor* A3(2) and *Streptomyces ambofaciens* ATCC 23877. Microbiology *152*, 3355–3366.

Barry, S.M., and Challis, G.L. (2009). Recent advances in siderophore biosynthesis. Curr. Opin. Chem. Biol. *13*, 205–215.

Boakes, S. (2002). New polyketide synthase in *Saccharopolyspora erythraea*. PhD Thesis. University of Cambridge.

Boakes, S., Oliynyk, M., Cortés, J., Böhm, I., Rudd, B.A., Revill, W.P., Staunton, J., and Leadlay, P.F. (2004). A new modular polyketide synthase in the erythromycin producer *Saccharopolyspora erythraea*. J. Mol. Microbiol. Biotechnol. *8*, 73–80.

Bode, H.B., Bethe, B., Hofs, R., and Zeeck, A. (2002). Big effects from small changes: possible ways to explore nature's chemical diversity. ChemBioChem *3*, 619–627.

Challis, G.L. (2005). A widely distributed bacterial pathway for siderophore biosynthesis independent of non ribosomal peptide synthetases. ChemBioChem *6*, 601–611.

Challis, G.L. (2008). Mining microbial genomes for new natural products and biosynthetic pathways. Microbiology *154*, 1555–1569.

Challis, G.L., and Hopwood, D.A. (2003). Synergy and contingency as driving forces for the evolution of multiple secondary metabolite production by *Streptomyces* species. Proc. Natl. Acad. Sci. USA *100*, 14555–14561.

Challis, G.L., Ravel, J., and Townsend, C.A. (2000). Predictive, structure-based model of amino acid recognition by nonribosomal peptide synthetase adenylation domains. Chem. Biol. *7*, 211–224.

Chipperfield, J.R., and Ratledge, C. (2000). Salicyclic acid is not a bacterial siderophore: a theoretical study. Biometals *13*, 165–168.

Clardy, J., Fischbach, M.A., and Walsh, C.T. (2006). New antibiotics from bacterial natural products. Nat. Biotechnol. *24*, 1541–1550.

Cortés, J., Velasco, J., Foster, G., Blackaby, A.P., Rudd, B.A., and Wilkinson, B. (2002). Identification and cloning of a type III polyketide synthase required for diffusible pigment biosynthesis in *Saccharopolyspora erythraea*. Mol. Microbiol. *44*, 1213–1224.

Crosa, J.H., and Walsh, C.T. (2002). Genetics and assembly-line enzymology of siderophore biosynthesis in bacteria. Microbiol. Mol. Biol. Rev. *66*, 223–249.

Custot, J., Boucher, J.-L., Vadon, S., Guedes, C., Dijols, S., Delaforge, M., and Mansuy, D. (1996). *N*-ω-hydroxyamino-α-amino acids as a new class of very strong inhibitors of arginases. J. Biol. Inorg. Chem. *1*, 73–82.

De Lorenzo, V., and Neilands, J.B. (1986). Characterization of *iucA* and *iucC* genes of the aerobactin system of plasmid ColV-K30 in *Escherichia coli*. J. Bacteriol. *167*, 350–355.

Dimise, E.J., Widboom, P.F., and Bruner, S.D. (2008). Structure elucidation and biosynthesis of fuscachelins, peptide siderophores from the moderate thermophile *Thermobifida fusca*. Proc. Natl. Acad. Sci. USA *105*, 15311–15316.

Dolence, E.K., and Miller, M.J. (1991). Synthesis of foroxymithine, a microbial fermentation product and angiotensin I converting enzyme inhibitor. J. Org. Chem. *56*, 492–499.

Dyda, F., Klein, D.C., and Hickman, A.B. (2000). GCN5-related *N*-acetyltransferases: a structural overview. Annu. Rev. Biophys. Biomol. Struct. *29*, 81–103.

Flett, F., Mersinias, V., and Smith, C.P. (1997). High efficiency intergeneric conjugal transfer of plasmid DNA from *Escherichia coli* to methyl DNA-restricting Streptomycetes. FEMS Microbiol. Lett. *155*, 223–229.

Flores, F.J., and Martin, J.F. (2004). Iron-regulatory proteins DmdR1 and DmdR2 of *Streptomyces coelicolor* form two different DNA-protein complexes with iron boxes. Biochem. J. *380*, 497–503.

Frank, B., Wenzel, S.C., Bode, H.B., Scharfe, M., Blöcker, H., and Müller, R. (2007). From genetic diversity to metabolic unity: studies on the biosynthesis of aurafurones and aurafuron-like structures in myxobacteria and streptomycetes. J. Mol. Biol. *374*, 24–38.

Gehring, A.M., Mori, I., and Walsh, C.T. (1998). Reconstitution and characterization of the *Escherichia coli* enterobactin synthetase from EntB, EntE, and EntF. Biochemistry *37*, 2648–2659.

Gu, L., Geders, T.W., Wang, B., Gerwick, W.H., Håkansson, K., Smith, J.L., and Sherman, D.H. (2007). GNAT-like strategy for polyketide chain initiation. Science *318*, 970–974.

Gust, B., Challis, G.L., Fowler, K., Kieser, T., and Chater, K.F. (2003). PCR-targeted *Streptomyces* gene replacement identifies a protein domain needed for biosynthesis of the sesquiterpene soil odor geosmin. Proc. Natl. Acad. Sci. USA *100*, 1541–1546.

Haas, H. (2003). Molecular genetics of fungal siderophore biosynthesis and uptake: the role of siderophores in iron uptake and storage. Appl. Microbiol. Biotechnol. *62*, 316–330.

Hsieh, Y.J., and Kolattukudy, P.E. (1994). Inhibition of erythromycin synthesis by disruption of malonyl-coenzyme A decarboxylase gene *eryM* in *Saccharopolyspora erythraea*. J. Bacteriol. *176*, 714–724.

Hu, J., and Miller, M.J. (1994). A new method for the synthesis of N^{δ}-acetyl-N^{δ}-hydroxy-L-lysine, the iron-binding constituent of several important siderophores. J. Org. Chem. *59*, 4858–4861.

Hunaiti, A.R., and Kolattukudy, P.E. (1984). Malonyl-CoA decarboxylase from *Streptomyces erythreus*: purification, properties, and possible role in the production of erythromycin. Arch. Biochem. Biophys. *229*, 426–439.

Imoto, M., Umezawa, K., Komuro, K., Sawa, T., Takeuchi, T., and Umezawa, H. (1987). Antitumor activity of erbstatin, a tyrosine protein kinase inhibitor. Jpn. J. Cancer Res. *78*, 329–332.

Kieser, T., Bibb, M.J., Buttner, M.J., Chater, K.F., and Hopwood, D.A. (2000). Practical *Streptomyces* Genetics (Norwich: The John Innes Foundation).

Kim, D.-W., Chater, K.F., Lee, K.-J., and Hesketh, A. (2005). Effects of growth phase and the developmentally significant *bldA*-specified tRNA on the membrane-associated proteome of *Streptomyces coelicolor*. Microbiology *151*, 2707–2720.

Knof, U., and von Zelewsky, A. (1999). Predicted chirality at metal centers. Angew. Chem. Int. Ed. Engl. *38*, 302–322.

Kohli, R.M., and Walsh, C.T. (2003). Enzymology of acyl chain macrocyclization in natural product biosynthesis. Chem. Commun. (Camb.), 297–307.

Konz, D., and Marahiel, M.A. (1999). How do peptide synthetases generate structural diversity? Chem. Biol. *6*, R39–R48.

Lautru, S., Deeth, R.J., Bailey, L.M., and Challis, G.L. (2005). Discovery of a new peptide natural product by *Streptomyces coelicolor* genome mining. Nat. Chem. Biol. *1*, 265–268.

Lautru, S., Oves-Costales, D., Pernodet, J.-L., and Challis, G.L. (2007). MtbH-like protein-mediated cross-talk between non-ribosomal peptide antibiotic and siderophore biosynthetic pathways in *Streptomyces coelicolor* M145. Microbiology *153*, 1405–1412.

Madduri, K., Waldron, C., and Merlo, C.J. (2001). Rhamnose biosynthesis pathway supplies precursors for primary and secondary metabolism in *Saccharopolyspora spinosa*. J. Bacteriol. *183*, 5632–5638.

Martínez, J.L., Herrero, M., and de Lorenzo, V. (1994). The organization of intercistronic regions of the aerobactin operon of pColV-K30 may account for the differential expression of the iucABCD and iutA genes. J. Mol. Biol. *238*, 288–293.

Milagres, A.M., Machuca, A., and Napoleão, D. (1999). Detection of siderophore production from several fungi and bacteria by a modification of chrome azurol S (CAS) agar plate assay. J. Microbiol. Methods *37*, 1–6.

Oliveira, P.H., Batagov, A., Ward, J., Baganz, F., and Krabben, P. (2006). Identification of erythrobactin, a hydroxamate-type siderophore produced by *Saccharopolyspora erythraea*. Lett. Appl. Microbiol. *42*, 375–380.

Oliynyk, M., Samborskyy, M., Lester, J.B., Mironrenko, T., Scott, N., Dickens, S., Haydock, S.F., and Leadlay, P.F. (2007). Complete genome sequence of the erythromycin-producing bacterium *Saccharopolyspora erythraea* NRRL23338. Nat. Biotechnol. *25*, 447–453.

Partida-Martinez, L.P., and Hertweck, C. (2007). A gene cluster encoding rhizoxin biosynthesis in "Burkholderia rhizoxina", the bacterial endosymbiont of the fungus *Rhizopus microsporus*. ChemBioChem *8*, 41–45.

Peano, C., Bicciato, S., Corti, G., Ferrari, F., Rizzi, E., Bonnal, R.J., Bordoni, R., Albertini, A., Bernardi, L.R., Donadio, S., and De Bellis, G. (2007). Complete gene expression profiling of *Saccharopolyspora erythraea* using GeneChip DNA microarrays. Microb. Cell Fact. *6*, 37.

Piel, J., Wen, G., Platzer, M., and Hui, D. (2004). Unprecedented diversity of catalytic domains in the first four modules of the putative pederin polyketide synthase. ChemBioChem *5*, 93–98.

Pohlmann, V., and Marahiel, M.A. (2008). Delta-amino group hydroxylation of L-ornithine during coelichelin biosynthesis. Org. Biomol. Chem. *6*, 1843–1848.

Rausch, C., Weber, T., Kohlbacher, O., Wohlleben, W., and Huson, D.H. (2005). Specificity prediction of adenylation domains in nonribosomal peptide synthetases (NRPS) using transductive support vector machines (TSVMs). Nucleic Acids Res. *33*, 5799–5808.

Rausch, C., Hoof, I., Weber, T., Wohlleben, W., and Huson, D.H. (2007). Phylogenetic analysis of condensation domains in NRPS sheds light on their functional evolution. BMC Evol. Biol. *7*, 78.

Revill, W.P., Bibb, M.J., and Hopwood, D.A. (1995). Purification of a malonyltransferase from *Streptomyces coelicolor* A3(2) and analysis of its genetic determinant. J. Bacteriol. *177*, 3946–3952.

Rowe, C.J., Cortés, J., Gaisser, S., Staunton, J., and Leadlay, P.F. (1998). Construction of new vectors for high-level expression in actinomycetes. Gene *216*, 215–223.

Rowe, C.J., Böhm, I.U., Thomas, I.P., Rudd, B.A.M., Foster, G., Blackaby, A.P., Sidebottom, P.J., Roddis, Y., Buss, A.D., Staunton, J., and Leadlay, P.F. (2001). Engineering a polyketide with a longer chain by insertion of an extra module into the erythromycin producing polyketide synthase. Chem. Biol. *8*, 475–485.

Sambrook, J., Fritsch, E.F., and Maniatis, T. (1989). Molecular Cloning: A Laboratory Manual (New York: Cold Spring Harbor Laboratory Press).

Schwarzer, D., Mootz, H.D., Linne, U., and Marahiel, M.A. (2002). Regeneration of misprimed nonribosomal peptide synthetases by type II thioesterases. Proc. Natl. Acad. Sci. USA *99*, 14083–14088.

Schwecke, T., Göttling, K., Durek, P., Dueñas, I., Käufer, N.F., Zock-Emmenthal, S., Staub, E., Neuhof, T., Dieckmann, R., and von Döhren, H. (2006). Nonribosomal peptide synthesis in *Schizosaccharomyces pombe* and the architectures of ferrichrome-type siderophore synthetases in fungi. ChemBioChem *7*, 612–622.

Schwyn, B., and Neilands, J.B. (1987). Universal chemical assay for the detection and determination of siderophores. Anal. Biochem. *160*, 47–56.

Sharman, G.J., Williams, D.H., Ewing, D.F., and Ratledge, C. (1995). Isolation, purification and structure of exochelin MS, the extracellular siderophore from Mycobacterium smegmatis. Biochem. J. *305*, 187–196.

Sieber, S.A., and Marahiel, M.A. (2005). Molecular mechanisms underlying nonribosomal peptide synthesis: approaches to new antibiotics. Chem. Rev. *105*, 715–738.

Stachelhaus, T., Mootz, H., and Marahiel, M. (1999). The specificity-conferring code of adenylation domains in nonribosomal peptide synthetases. Chem. Biol. *6*, 493–505.

Stegmann, E., Rausch, C., Stockert, S., Burkert, D., and Wohlleben, W. (2006). The small MbtH-like protein encoded by an internal gene of the balhimycin biosynthetic gene cluster is not required for glycopeptide production. FEMS Microbiol. Lett. *262*, 85–92.

Steller, S., Sokoll, A., Wilde, C., Bernhard, F., Franke, P., and Vater, J. (2004). Initiation of surfactin biosynthesis and the role of the SrfD-thioesterase protein. Biochemistry *43*, 11331–11343.

Summers, R.G., Ali, A., Shen, B., Wessel, W.A., and Hutchinson, C.R. (1995). Malonyl-coenzyme A: acyl carrier protein acyltransferase of *Streptomyces glaucescens*: a possible link between fatty acid and polyketide biosynthesis. Biochemistry *34*, 9389–9402.

Sun, Y., Hong, H., Samborskyy, M., Mironenko, T., Leadlay, P.F., and Haydock, S.F. (2006). Organization of the biosynthetic gene cluster in *Streptomyces* sp. DSM 4137 for the novel neuroprotectant polyketide meridamycin. Microbiology *152*, 3507–3515.

Umezawa, H., Aoyagi, T., Ogawa, K., Obata, T., Iinuma, H., Naganawa, H., Hamada, M., and Takeuchi, T. (1985). Foroxymithine, a new inhibitor of angiotensin-converting enzyme, produced by actinomycetes. J. Antibiot. (Tokyo) *38*, 1813–1815.

Wandersman, C., and Deleplaire, P. (2004). Bacterial iron sources: from siderophores to hemophores. Annu. Rev. Microbiol. *58*, 611–647.

Weissman, K.J., Hong, H., Oliynyk, M., Siskos, A.P., and Leadlay, P.F. (2004). Identification of a phosphopantetheinyltransferase for erythromycin production in *Saccharopolyspora erythraea*. ChemBioChem *5*, 116–125.

Xu, Y., Orozco, R., Wijeratne, E.M., Gunatilaka, A.A., Stock, S.P., and Molnár, I. (2008). Biosynthesis of the cyclooligomer depsipeptide beauvericin, a virulence factor of the entopathogenic fungus *Beauveria bassiana*. Chem. Biol. *15*, 898–907.

Xu, Y., Orozco, R., Wijeratne, E.M., Espinosa-Artiles, P., Gunatilaka, A.A., Stock, S.P., and Molnár, I. (2009). Biosynthesis of the cyclooligomer depsipeptide bassaniolide, an insecticidal virulence factor of *Beauveria bassiana*. Fungal Genet. Biol. *46*, 353–364.

Yeats, C., Bentley, S., and Bateman, A. (2003). New knowledge from old: in silico discovery of novel protein domains in *Streptomyces coelicolor*. BMC Microbiol. *3*, 3.

Yin, X., and Zabriskie, T.M. (2006). The enduracidin biosynthetic gene cluster from *Streptomyces fungicidicus*. Microbiology *152*, 2969–2983.

Zerikly, M., and Challis, G.L. (2009). Strategies for the discovery of new natural products by genome mining. ChemBioChem *10*, 625–633.

Zhang, Y., Buchholz, F., Muyrers, J.P.P., and Stewart, A.F. (1998). New logic for DNA engineering by recombination in *E. coli*. Nat. Genet. *20*, 123–128.

Note Added in Proof

While this manuscript was under review, an identical structure for erythrochelin has been reported independently (Robbel, L., Knappe, T. A., Linne, U., Xie, X, and Marahiel, M. A. (2009). FEBS J., doi: 10.1111/j.1742-4658.2009.07512.x).